Research Article

Studies on toxicity of noscapine loaded hydroxyapatite nanoparticles

Hava KÖLEMEK[1] , **İbrahim BULDUK[2]** , **Yavuz ERGÜN[3]** , **Safiye Elif KORCAN[4]** ,
Recep LİMAN[1] , **Muhsin KONUK[5,*]** , **Funda Karabağ ÇOBAN[1]**

[1]*Department of Molecular Biology and Genetics, Faculty of Arts and Sciences, Uşak University, Uşak, 64300, Türkiye*
[2]*Uşak University, School of Health Sciences, Uşak, 64300, Türkiye*
[3]*Department of Chemical Engineering, Faculty of Arts and Sciences, Uşak University, Uşak, 64300, Türkiye*
[4]*Uşak University, Health Care Vocational School, Uşak, 64300, Türkiye*
[5]*Üsküdar University, Biotechnology Research and Application Centre, Istanbul,34662, Türkiye*

ABSTRACT

In this study, we loaded noscapine (NOS) into the hydroxyapatite nanoparticles (HAPs) and determine the release of NOS in acidic pH to extend its circulation time in the bloodstream. For the aim, NOS loaded HAP nanoparticles were obtained to characterize typical functional groups and to examine the size, the morphology of these nanoparticles, Fourier Transform Infrared Spectroscopy (FTIR), Scanning Electron Microscopy (SEM), and Energy Dispersive X-ray (EDX), Transmission Electron Microscopy (TEM) analysis were employed. Intercalary prepared HAPs are characterized by X-ray diffraction. The amount of NOS trapped in the HAPs was determined by High-performance liquid chromatography (HPLC). Comet Assay also evaluated the DNA damage of NOS-loaded hydroxyapatite nanoparticles (HAPs). The significance levels in different treatment groups were analyzed using the Duncan multiple range tests in SPSS 23.0 version for Windows software. P<0.05 was set as statistical significance. In the characterization studies, it was observed that NOS release increased linearly in acidity over time. The toxicities of the HAP and NOS-loaded HAP were also evaluated. NOS-loaded HAP was found to be reducing the harmful effects. Therefore, HAP seems to be an interesting alternative for further studies on noscapine transport and dose-dependent toxicity reduction.

Cite this article as: Kölemek H, Bulduk İ, Ergün Y, Korcan SE, Liman R, Konuk M, Çoban FK. Studies on toxicity of noscapine loaded hydroxyapatite nanoparticles. Sigma J Eng Nat Sci 2023;41(4):824–836.

INTRODUCTION

Noscapine (NOS) is an alkaloid of phthalide isoquinoline alkaloid present in the opium poppy family of plants. This drug has been extensively studied for its effectiveness against different types of cancer (lymphoma, melanoma, prostate, lung cancers) [1-3]. NOS inhibit cancer tumor by interfering with microtubule function at the cellular level, thereby arresting cell growth and inducing apoptosis [4].

Recent studies have shown that NOS can be used not only for cancer therapy but also for many other treatments.

---

*Corresponding author.
*E-mail address: mkonuk@gmail.com

This paper was recommended for publication in revised form by Regional Editor Banu Mansuroglu

Jayaraj et al. findings imply that noscapine protects dopaminergic neurons by lowering synuclein expression and activating the mammalian target of the rapamycin (mTOR) pathway, which results in fewer autophagic vacuoles being formed and increased autophagy flux [5]. Ebrahimi reported that noscapine therapy might help reduce bradykinin-mediated cytokine release due to ACE2 inhibition by SARS-CoV-2. This can reduce tissue damage, particularly in the lungs, shorten patients' recovery time, and potentially save lives [6]. In a study conducted in individuals with moderate to severe ACEI-induced cough to determine the therapeutic efficacy of NOS, it was determined that within 2-4 days, 90 percent of the individuals recovered from coughing, and angiotensin-converting enzyme inhibitors (ACEI) medication was allowed to continue [7]. Further research suggested that NOS may be useful in shielding neuronal cells and tissues from ischemia and oxidative damage [8,9]. NOS has recently received a lot of attention as a potential antibacterial target for new drug development. The bacterial cell wall protein FtsZ is a close homolog of eukaryotic tubulin and possesses the tubulin 7-amino-acid motif. The FtsZ protein encourages the creation of a ring between freshly formed progeny cells in the division zone [10].

It has been reported that NOS has the highest level in plasma within 2-3 hours when administered orally and it cannot be detected after 6 hours [11-13]. While it has a low toxicity profile, it has impeded its production as a commercially available medication due to the high dose demand and poor bioavailability [3]. Some alternative methods have been identified for drug delivery, including nanoparticles [14,15] and the researchers are still ongoing to find the most effective mechanism to resolve the pharmacokinetic limitations.

Nanoparticles are important scientific tools used in a variety of biotechnological and pharmacological applications due to their physicochemical properties associated with residue sizes. Nanomaterials that pose no health risks and are not cytotoxic in nature have become a hot topic recently [16]. Because of their large surface area and very small size, nanoparticles generate reactive oxygen species that directly attack DNA and thus cause oxidative damage. The different nanotoxic effects that different nanomaterials can have are still not fully known and research on toxic mechanisms continues [17].

Biomaterials based on hydroxyapatite have been clinically used in orthopedic and dental repair since the 1970s. Often commonly accepted surface adjustment with a hydroxyapatite coating on prosthetic metal implants to improve bone integration. In recent years, hydroxyapatite nanoparticles (HAPs) are capable of inhibiting proliferation and inducing apoptosis in various types of cancer cells such as colon, osteosarcoma, hepatic, breast, and gastric cancer cells like NOS [18]. There are many things to the inhibiting proliferation and inducing apoptosis cancer cells process. First, increased intracellular oxidative stress and impaired endoplasmic reticulum function. Second, tumor cell phagocytosis, and hence the nanoparticle's cytoplasmic internalization, was greater than that of normal cells. Finally activated mitochondrion-mediated apoptosis pathways were observed preferentially in HAP-treated tumor cells [18-22]. Importantly a composite scaffold with zoledronic acid loaded with HAP has also been developed for the recovery of tumor-induced bone defects [23]. Far less is known about the influence of HAP in vivo on antitumors, and the exact mechanism has not yet been investigated. Among the drug carrier systems, hydroxyapatite is of great interest because of its biocompatibility [24]. The recent advances in the structural characterization at the nanoscale level and in the colloidal stabilization of apatite nanocrystals have opened new perspectives on their uses as drug carriers in nanomedicine.

Both NOS and HAP have an antitumor effect. Also, NOS is used as a pain reliever in cancer patients. Therefore, this study aims to incorporate NOS into the HAPs and determine the release of NOS in acidic pH of the stomach acidity to extend its circulation time in the bloodstream and investigate any possible genotoxicity effects of NOS loaded HAPs on DNA.

MATERIAL AND METHODS

Poppy capsules were obtained from Afyon Alkaloid Factory Operation Directorate in Afyonkarahisar province. Capsules were broken and separated from the seeds and dried in a dark room at room temperature for 15 days and then milled to 80 mesh grain size in the mill. After Ultrasonic Supported Methanol Extraction, the extracts were filtered through a White-band filter paper (MN 617 Ø 110 mm). The Folin Ciocalteu method was used to determine the total amount of phenolic substances in methanol extracts by following the method of Gamez et al [25]. The total flavonoid content of the poppy capsules was determined by the aluminum chloride colorimetric method [26]. 2,2-Diphenyl-1-picrylhydrazyl (DPPH) method was also used to determine the free radical removal activity of the methanol extracts. The percentage of inhibition of the reaction of DPPH radical was calculated using the following formula.

% Inhibition = [(AC-AE) / AC] X 100

AC: Absorption of Control; AE: Absorbance of example.

After drawing a linear regression curve, antioxidant concentrations caused 50% inhibition [EC_{50} (µg/ml)] was determined by using this percentage inhibition graph.

NOS Extraction of Poppy Capsules

250 g of dried and ground capsules were kept in a solution of 0.1 M HCl for one day, then 500 mL of ethanol was added and 10-15 minutes of solid-liquid extraction was performed on the mechanical stirrer. This procedure was repeated three times. The mixture was filtered through white tape filter paper. The ethanol in the filtrate was

evaporated in a rotary evaporator under a vacuum at 40° C to give concentrated extracts.

Purification of the extracts was carried out in three steps. In the first step, activated carbon (10 g into 500 mL of extract) was added to remove vegetable-origin color pigments. The mixture was then stirred for 30 minutes at 60 °C on a magnetic stirrer and filtered with a white band filter paper. In the second step, diatomaceous earth was added to remove plant-induced turbidity and to obtain a clearer solution. After adding 10 g of diatomaceous earth to the concentrated extract, it was stirred for 30 minutes at 60 °C in a magnetic stirrer and passed through the filter paper. In the final step, liquid-liquid extraction with petroleum ether (1:1) was carried out to remove plant-derived oil, wax, and tannin. As a result of the process, concentrated NOS extracts were confined to the nanoparticles [27].

Synthesis of Hydroxyapatite Nanoparticle (HAP) By Solution-Precipitation Method

HAP was synthesized by using the solution-precipitation method. 41 g of $Ca(NO_3)_2$ was dissolved in 200 mL of ethanol. We used ethanol instead of water to fully dissolve $Ca(NO_3)_2$ [28] and 11.8 g $(NH_4)_3PO_4$ was dissolved in 250 ml of water, separately, then these two solutions were mixed on a magnetic stirrer at 60 °C for 4 hours. After leaving it overnight, 100 mL $(NH_4)_3PO_4$ solution was placed on the magnetic stirrer (60 °C 250 rpm) to form the empty HAPs. 100 mL of $Ca(NO_3)_2$ solution was added dropwise over 1 hour. After the addition was complete, stirring was continued at 60 °C for another 4 hours. Their amount was doubled for sol-gel formation (82 g of $Ca(NO_3)_2$ and 23.6 g $(NH_4)_3PO_4$). After filtering with filter paper, white nanoparticles were obtained. These particles were then washed three times with water and dried at 105 °C for 4 hours [29]. To load NOS into the HAPs, 40 mL of concentrated NOS extract (27,500 ppm) was added to 100 mL $(NH_4)_3PO_4$ solution and shaken at 60 °C and 250 rpm. 100 ml of $Ca(NO_3)_2$ solution was then added to the mixture dropwise over 1 hour. The resulting product, synthesis by the solution-precipitation method and the used for SEM and TEM analyzes.

Determination of NOS Content by HPLC Analysis

Determination of both presence and amount of the NOS after the extraction and purification steps were realized by the HPLC technique. The details of the analysis are given in Table 1. 200 mg of the dried nanoparticle loaded with noscapine was weighed. 20 mL of 0.1 M HCl was added. It was kept in the ultrasonic bath for 15 minutes and dissolved. The obtained solution was analyzed by HPLC and the amount of noscapine in the loaded nanoparticle was determined. In HPLC analysis, 0.1% TEA was used to correct the parameters of the NOS peak such as tailing and symmetry.

Characterization of Hydroxyapatite (HAP)

FTIR analysis was performed to determine the different functional phosphate and carbonate groups inside the synthesized HAPs. Analysis of FTIR was performed after HAPs dried at 105°C. Spectrum Two Perkin Elmer brand FTIR Spectrometer versions were used in FTIR analyses. The FTIR spectra of the samples were taken in the frequency range of 500-4000 cm-1. FTIR analyzes of the samples were performed in triplicate. SEM analysis was carried out to assess the morphological and grain sizes of the synthesized nanoparticles. In this study, the Phenom brand ProX model SEM tool was used. TEM analysis was performed to clarify the size, shape, morphology, and structure of the nanoparticles. JEOL JEM-2100 Transmission Electron Microscope device was used in the analysis. The X-Ray Diffraction Device (RIGAKU RINT 2000) was used to determine the crystalline and amorphous properties of the nanoparticle. Analyses to measure the viscosity of the colloidal hydroxyapatite powders in the solvent, the zeta (ς) potential of the surface charge, and the dielectricity of the solvent were carried out on a Malvern Zetasizer Nanozs 3600 branded device. Pure water was used to prepare low concentrations of samples for Zetasizer analysis (at 23-24 °C and pH 6.7). The experiments were carried out with a particle size range of 3-10 nm sensitivity.

Drug Release Experiment

It was set up as a simulation medium in vitro to mimic the acidic condition of the stomach to investigate the release of NOS from uploaded nanoparticles. For this, 200

Table 1. HPLC analysis conditions

	Gradient conditions		
Column: ACE brand (5 µm, 150 mm X 4,6 mm I.D.)	**Time**	**Mobile phase -A (%)**	**Mobile phase -B (%)**
Mobile Phase-A: 5% acetonitrile water solution	0	90	10
Mobile Phase-B: 97.9% acetonitrile, 2.0% glacial acetic acid, 0.1% TEA	5	85	15
Flow rate: 1 mL / min	10	80	20
Column temperature: 30°C	20	65	35
Injection volume: 50 µL	30	90	10
Detection wavelength: 284 nm			
Analysis time: 30 min			

mg of NOS-loaded HAPs was weighed in a beaker and 20 mL of NaCl/HCl, (pH 1.2) solution was added to it, then it was placed in a shaking incubator (at 37 °C, 70 rpm). 2 mL of a sample from the mixture was taken every five hours to analyze on HPLC to define the amount of the released NOS as mentioned by Gün [30].

Comet Assay

The blood samples were collected from a healthy and non-smoking young donor at the age of 28. Leukocytes were isolated over Histopaque 1083 gradients by centrifugation at 2100 rpm for 20 min at 15 °C. The comet assay was performed under alkaline conditions according to Singh et al. [31]. Isolated human leukocytes (100 μL) were incubated with 100 μL different concentrations of HA and NOS loaded HA (5, 10, and 25 mg/mL) [16,17,32] for 1 h at 37 °C. Positive (30 mM H_2O_2) and solvent control (1XPBS) were also included. Following the incubation, leucocytes were at 1600 rpm for 10 min at 25 °C. While supernatant was used for Total antioxidant status (TAS) and total oxidant status (TOS) determination, the pellet was used for Comet assay. The Comet assay protocol was carried out by following the method of Avuloglu-Yilmaz et al. Each pellet was then resuspended with 100 μL of PBS. 80 μL of 0.8% LMA melted at 37±0.5 °C was mixed with 20 μL of cell suspension, then immersed in 1.5% NMA solution and spread on slides coated with agar and covered with a coverslip. Polymerization of agar by keeping it on a frosted surface for 5 minutes provided. The coverslip on the agar was carefully removed. The slides were immersed in the cold lysis solution prepared previously and kept in the refrigerator and kept in the refrigerator for at least 1 hour. Then, for the electrophoresis process, the electrophoresis tank was filled with cold electrophoresis solution and the slides were placed in the electrophoresis tank and kept without applying current for 20 minutes. Electrophoresis was applied for 20 minutes by applying 25 V and 300 mA current. After the electrophoresis process is finished, the slides are taken for 5 minutes. kept in distilled water. Afterward, the slides were kept in a neutralization buffer solution for 15 minutes. Staining was achieved by adding 60 μL of 20 μg/mL ethidium bromide solution to the slides. [33]. The analysis of comet scores was calculated as described by Cigerci et al. [34]. Briefly, fifty comets (50 comets/slide) were visually scored as belonging to one of five classes (0-no damage, 1-light damage, 2-moderate, 3-severe damage, 4-complete damage) using a fluorescence microscope. Therefore, the overall score for 50 comets can range from 0 (all undamaged) to 200 (all damaged). The percentage of damaged cells was calculated. The Arbitrary Unit used to express the degree of DNA damage is calculated as the following equation):

$$Arbitrary\ Unit = \sum_{i=0}^{4} Ni \times i$$

Ni = Number of cells in i degree; i = degree of damage (0, 1, 2, 3, 4).

Measurement of Total Oxidant Status and Oxidative Stress Index

TOS and TAS were determined spectrophotometrically using Rel Assay Diagnostic kit RL0024 and RL0017 reading at 530 nm. and 660 nm., respectively by Elisa Thermo Scientific.

A hydroxyl radical is produced by this method when using Rel Assay Diagnostic kit RL0017. The hydroxyl radical is the strongest biological radical. The iron ion solution in reagent 1 is mixed with hydrogen peroxide in reagent 2. The test has >97% excellent precision values. Results are expressed as millimoles of Trolox equivalents per liter. The oxidants present in the sample oxidize the ferrous ion o-dianisidine to the ferrous ion when using Rel Assay Diagnostic kit RL0024. In the oxidation reaction, glycerol networks, which are abundant in the reaction medium, are grown. The ferric ion forms a colored complex with an acidic model xylenol orange. Color-measured spectrophotometrically. Results are expressed as micromolar apparent peroxide equivalents per liter (micromole H_2O_2 eq/L) [35,36].

TAS and TOS value was calculated according to the following formula;

TOS: (ΔAbsSample) / (ΔbsStandard) X Conc. of standard

TAS: [(ΔAbs H_2O) - (ΔAbs Sample)) / (ΔAbsH$_2$O) - (ΔAbs Standart)].

The oxidative stress index (OSI): TOS / TAS.

Statistical Analysis

The comet scores were presented as means ± standard deviation (± SD). The significance levels in different treatment groups were analyzed using the Duncan multiple range tests in SPSS 23.0 version for Windows software. $P < 0.05$ was set as statistical significance.

RESULTS AND DISCUSSION

There are several papers focused on long-lasting effective drug formulations in the last three decades. This could be achieved by keeping the constant concentration of the drug in bodily liquids to make them more effective against the diseases fought. One of the benefits of these new drugs is that they have fewer adverse and toxic/allergic effects [37]. HAP is one of the major contents of the bone and tooth tissues and has natural characteristic features such as biocompatibility, biodegradation, bio-solubility, osteogenesis, osteoconductivity, and osteoinductivity [38-40]. HAP nanoparticles are used in drug administration due to their solubility in vivo and good relations with the cellular membranes. They have also been able to inhibit the cancer tumor growth as reported by Liu et al.; Uskovic, and Lafisco et al. [41-43].

Nascopine is an isoquinoline alkaloid, an antitussive agent obtained from Opium, and has been extensively evaluated over the past two decades and has been found to have minimal toxicity and no effect on innate humoral and adaptive immunity. Since it is a tubulin-binding agent, it has been studied as a possible anti-cancer molecule [44,45]. It has also no sedative, addicting, or exciting effect when compared to other opium molecules. Additionally, it can be given orally while other alkaloids administrated do not.

In this study, we aimed to slow the release of NOS by removing it from opium capsules and loading it into HAP nanoparticles in order to keep the concentration of NOS in the bloodstream at a constant level and reduce its possible dose-related toxicity. The determination of the amount of NOS in the extracts was made by HPLC analysis. FTIR analyzes were used for the characterization of empty and NOS-loaded HAPs. The HPLC analysis method was validated. LOD, and LOQ values are 0.367 ppm and 1,100 ppm, respectively (Figure 1).

For this, after extracting NOS from the opium capsules, the TPC, TFC, and EC50 values were determined in the extract (Table 2). The total amount of phenolic compounds in the extract samples is given as gallic acid equivalent (GAE). The methanolic solution of the gallic acid was used to draw the calibration curve. The amount of phenolic substances was calculated using the equation obtained from this graph (y = 98.316x + 39.945) (R^2 = 0.99999). The total amount of flavonoids in the extract samples is given as quercetin equivalent (QE). The equality obtained from

the standard graph was used to determine the quantity of the flavonoids in the extracts (y = 2438.6x-0.2189) (R^2 = 0.9998). DPPH radical reducing activity of the extract was expressed as Inhibition percentage by using the equilibrium: Inhibition % = [(AK-AÖ)/AK] X 100 (AK: Absorption of Control; AÖ: Absorbance of example) (Table 2). As seen in Table 2, the EC50 values decrease, sweep activity of DPPH radical increases. Our results showed that the Opium capsules not only reached NOS but also have 6.9±0.91 mg GAE/gr of Phenolics, and 29.77±1.225 mg QE/1 gr flavonoid contents. The NOS amount equivalent to the EC50 value is 0.93 µg (Table 2).

Regarding HAP, although Feng et al. [46] reported that they observed $(PO_4)^{3-}$, $CO_3{}^{2-}$, OH^-, and water-based functional groups on HAP nanoparticles; we were unable to see groups in our newly synthesized HAP nanoparticles. These findings are detailed in Table 3 with a comparison of Feng et al.'s results [46]. As seen in Figure 2A, the $(PO_4)^{3-}$ bands on empty HAP were observed as 524, 562, 886, 993, 1060 ve 1124 cm^{-1}. The peak at 1346 cm^{-1} resembles $CO_3{}^{2-}$ ions which could be because of the adsorption of atmospheric CO_2 as explained by Cengiz [47]. The FTIR spectrum of NOS reveals numerous sharp bands that are primarily due to alkaloid ring system deformation and stretching vibrations. NOS also shows a powerful band at 1759 that can be identified with the stretching vibration C = O, while the stretching modes – C – O – C – can be found at 1029 cm^{-1} [15]. NOS loaded HAP gave the $(PO_4)^{3-}$ peaks at 519, 575, 658, 987, 1054 ve 1118 cm1. In Figure 2B, the 3539
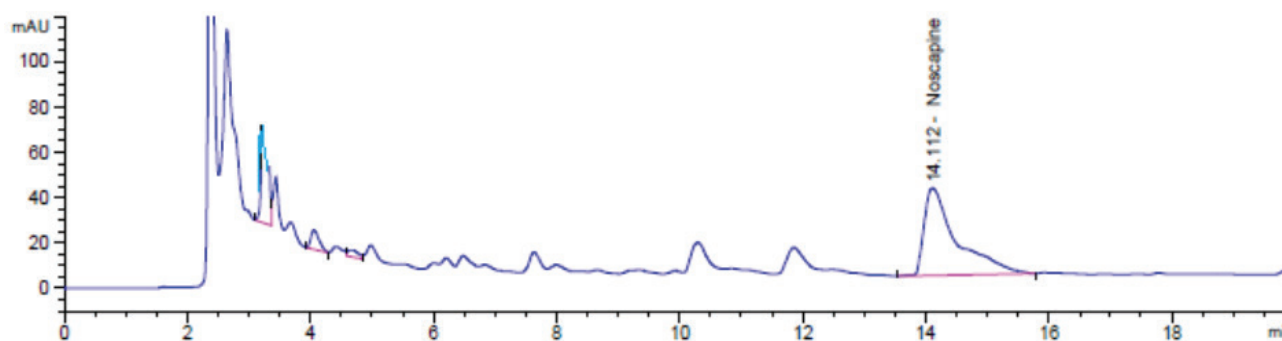
LOD: 0.367 ppm, LOQ: 1.100 ppm

Figure 1. HPLC chromatogram of the extract.

Table 2. Shows various results of chemical analysis of poppy capsules extracts and the amount of Noscapine

Chemical analysis	Results	Sample	Noscapine (ppm)
TPC	6.90±0.91 mg GAE/1g	Capsule	176
TFC	29.77±1.225 mg QE/1g	Extracts	147.1
EC$_{50}$ (The amount of NOS in the extract)	28 µL ±0.023 (0.93 µg)	Conc. extracts	2749.9
		HAP nanoparticles	12.7

Abbreviations: TPC: Total Phenolic Content, TFC: Total Flavonoid Content

peak resembles OH⁻ tension and the 1201 peak resembles $(CO_3)^{2-}$ ions possibly adsorbed from the air. As a result of point analysis, Ca and P ions were detected in unloaded HAP. These ions in the structure of hydroxyapatite $[Ca_5(PO_4)^3(OH)]$ were proof that the desired HAP is formed.

The structure of NOS $(C_{11}H_{17}NO_3)$ contains nitrogen ions. As a result of the SEM point analysis, the determination of the nitrogen and carbon with loaded particles has shown that NOS was loaded into HAP (Fig. 3A). The obtained solution was analyzed by HPLC and

the encapsulation efficiency was determined as 0.127 %. Spherical shape HA nanoparticles were observed to be average particle size distribution ranging from 10-100 nm at SEM analyzes (Fig. 3B). It was determined that this ratio increases when sintered. Kong et al, [48] reported the mechanisms of involvement of biomolecules on the surface of HAP particles that therapeutic agents can interact with the surface of the nanoparticles either through detachable covalent connections or the other through physical interactions such as electrostatic, hydrophobic/hydrophilic and
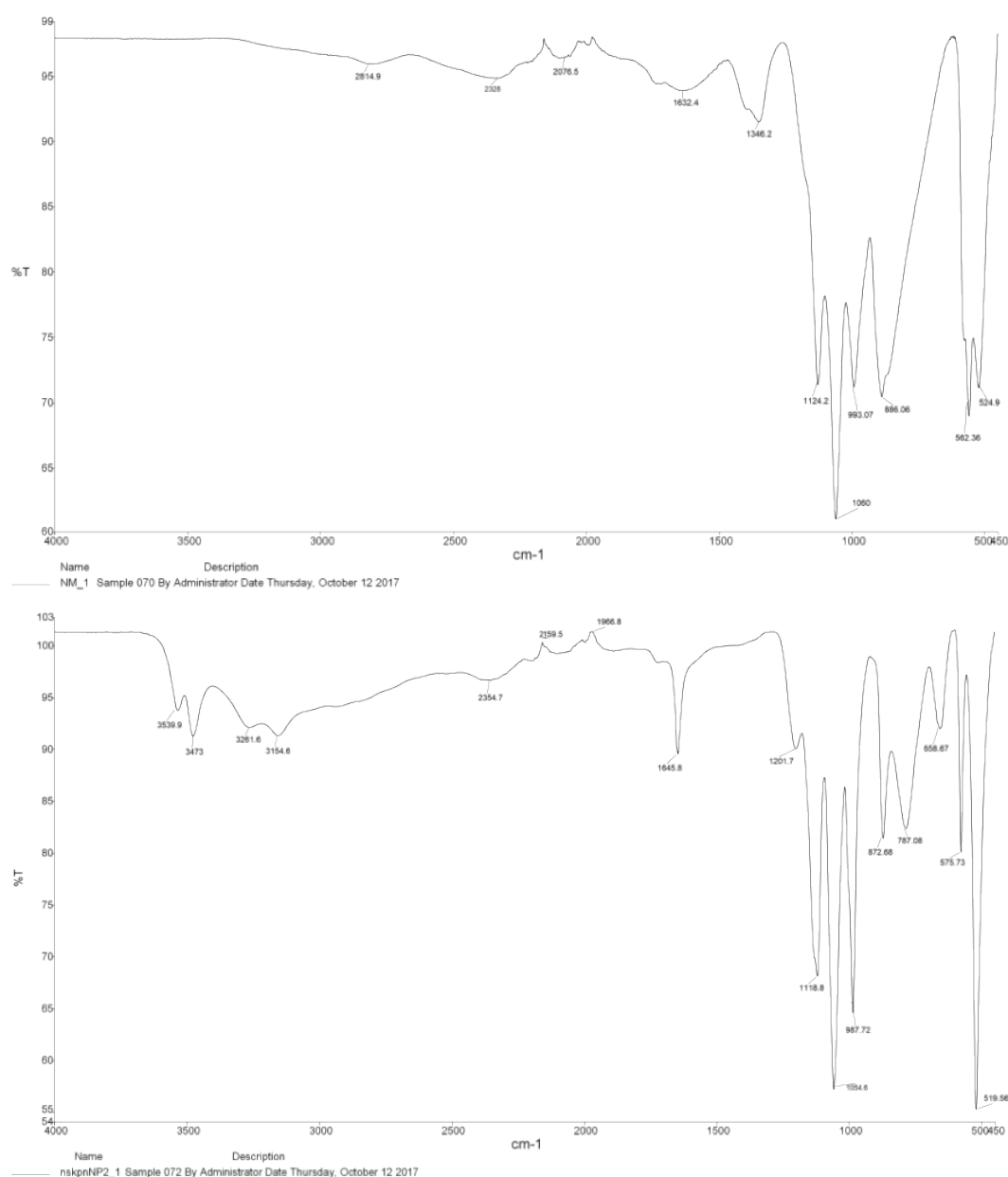
(A) To determine the functional phosphate and carbonate groups, synthesized HA, and (B) noscapine loaded HA (HAP) were subjected to FTIR analysis. The frequency zones were observed as 500-3500 cm⁻¹ in FTIR spectra. The dried particles at 105 ˚C were used.

**Figure 2.** HA (A) and NOS-loaded HA (B) FTIR spectra.
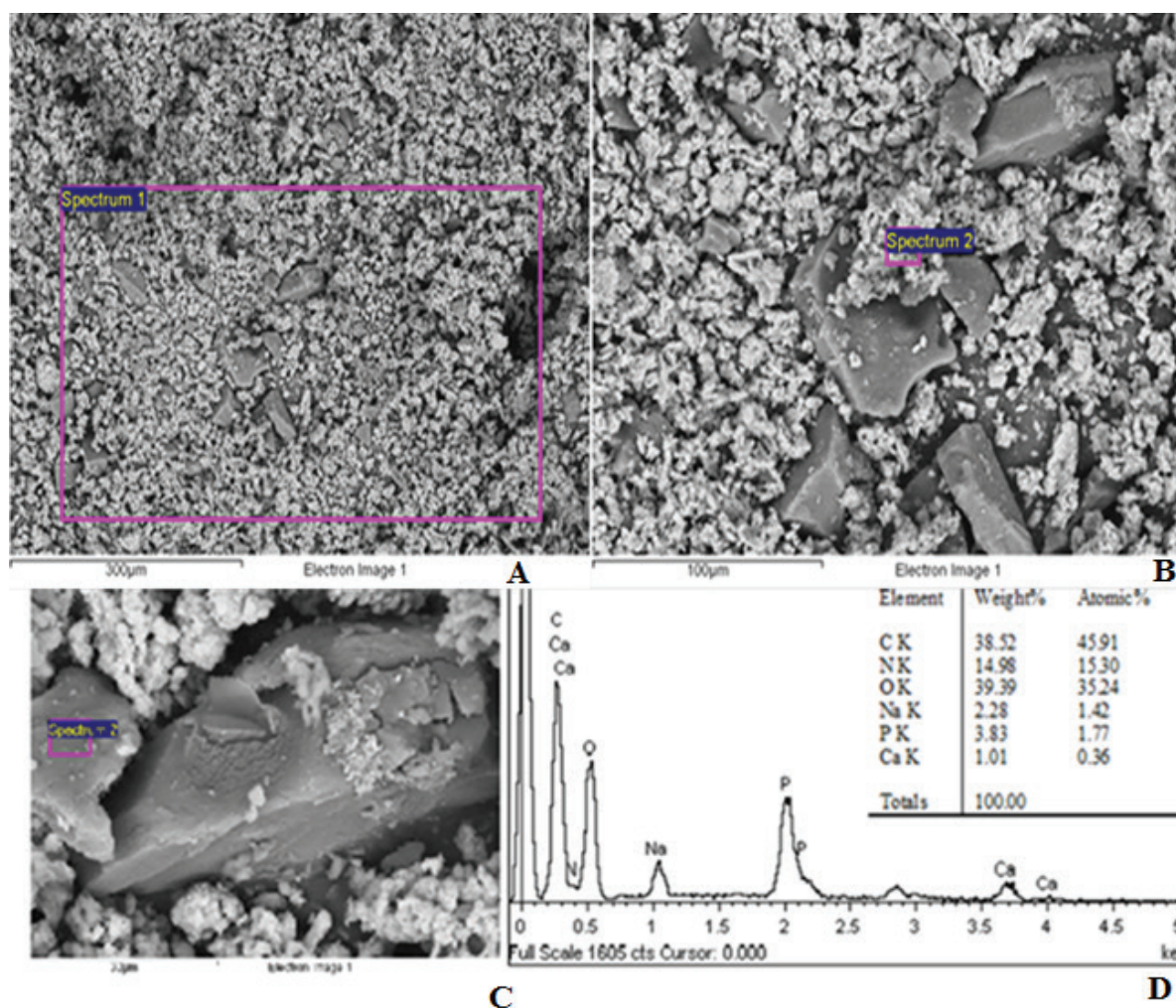
A: 300 µm, B: 200 µm, C; 22 µm, D: Element analysis of noscapine loaded HAPs.

Figure 3. Scanning Electron Microscopy SEM analysis of NOS loaded HA nanoparticle and morphological properties of the NPs.

affinity ones can lead to coupling of drug molecules with the surfaces of nanoparticles.

It was possible to see the element samples entering the chemical structure of HAP and NOS in the EDX analysis taken over the SEM image (Figure 3). The adsorption of polyvalent or surfactant oppositely charged ions of colloidal hydroxyapatite powders in the solvent to the surface may cause the ς zeta potential of the surface charge to change in the opposite direction, or the adsorption of the surfactant same charged ion may create an adverse situation. Due to the addition of ammonium hydroxide (NH_4OH) which is used for dispersant and pH adjustment in the solution, the stability of the solution has increased due to the increase of the zeta potential. It was observed that the viscosity increased very rapidly depending on the time in the sol without ammonium hydroxide added, while the left with ammonium hydroxide was observed to decrease with time.

In the experiment conducted to determine these effects, the results are given in Table 4. While Whitlockite $Ca_3(PO_4)_2$ and Hydroxyapatite $Ca_5(PO_4)3(OH)$ samples formed by sintering at 500-550 °C temperature are seen, Amorphous calcium phosphate $Ca_8H_2(PO_4)6(H_2O)_5$ and Hydroxyapatite $Ca_{10}(PO_4)6(OH)_2$ are formed in non-sintered samples. XRDs related to these are given in Figure 5. According to XRD results, the properties of the nanoparticles were amorphous In the formation of HAPs prepared by the sol-gel method, grain size, zeta positivity, and dispersion (disperse) are very important in terms of stability and efficiency of the solution [49]. As the surface area of HAP particles well dispersed in the solution will increase, it makes it more efficient in terms of NOS adhesion in the solution and entering the structure. The higher zeta potential in HAP grain surfaces with dispersant additive plays a role in increasing productivity (Table 4). The addition of dispersant prevented the grain to remain thinner by preventing the grain size in the Zeta potential.
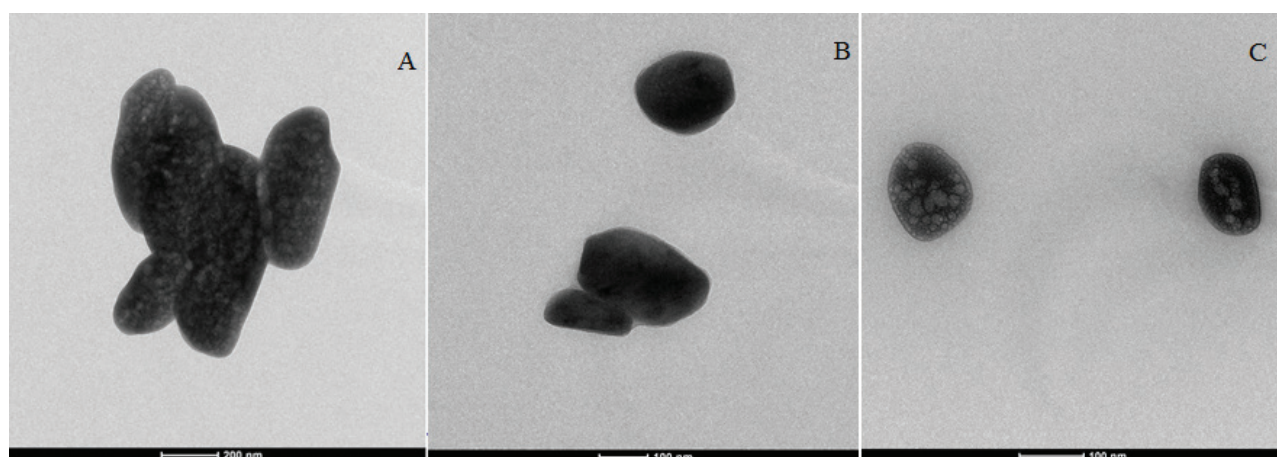
A: 200nm, B and C; 100nm. Transmission Electron Microscopy (TEM) was used to image the methanol homogenized NPs after keeping them 1 h in an ultrasonic bath.

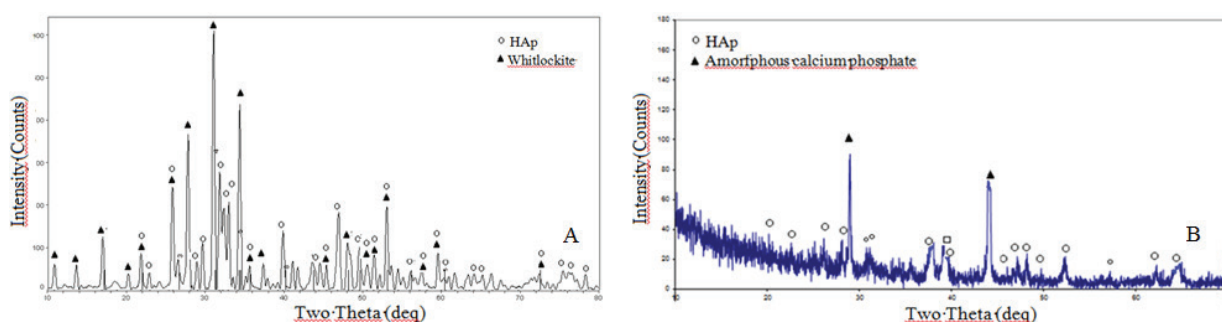**Figure 4.** TEM analysis of Spherical shape NOS loaded HA nanoparticle.

Figure 5. XRDs of NOS loaded HAPs at whitlockite and amorphous calcium phosphate.

Table 3. FTIR analysis of Noscapine Loaded Hydroxyapatite Nanoparticles and Hydroxyapatite Nanoparticles

| Sample	OH– stretching	The water associated with HAP	$(CO_3)_2$ Ion Peaks	The phosphate group,	Triply degenerated vibration of the P−O bond of the phosphate group	Nondegenerated symmetric stretching mode, of the P−O bond of the phosphate group, PO4.	Noscapine: sharp bands between 700-1500 cm^{-1}
Koutsopoulos, 2002	342, 631, 3572 cm^{-1}			1087, 1072–1032, 601, 571, and 474	1046 and 1032	962 cm−1	
Cimdina and Borodajenko, 2012	630 , 1650 3420, 3500, 3540, 3570		870 , 873, 880, 1450; 1460, 1530, 1640, 2000-2300,	460, 555, 560, 600, 602, 960, 1000 - 1100 1020 -1120 1040	875 and 880		
Feng et al. 2006	3571	3430 and 1632	1547, 1457 and 1415	1087, 1032, 602, 566 and 471		961	
Reference HAP	3564	3410 and 1638	-	1120, 1096, 617, 579 and 477	1030		
NOS-loaded HA	3539	3473 and1645	2354 and 2159	1118, 1054, 987, 658, 575, 519			1118, 1054, 987, 658, 575, 519
HA	-	1632	2814,2328 and 2076	1124, 1060, 993, 886, 562 and 524			

Abbreviations: HAP: Hydroxyapatite nanoparticle, HA: Hydroxyapatite, NOS: Noscapine OH− stretching vibration, a phosphate group, and $(CO_3)^2$ ıon peaks evidences the formation of HAP. Peaks of 1118, 1054, 987, 658, 575, 519 indicate the presence of noscapine.

Table 4. Zeta Potential and Solution Conductivity of HAPs in ammonium hydroxide free and ammonium hydroxide free solution

	Ammonium Hydroxide Free Solution (Without Dispersive Additive)	Ammonium Hydroxide Solution (With dispersant)
Zeta Potential (mV)	40.1	56.9
Zeta Distribution (mV)	138	194
Solution Conductivity (mS / cm)	15.8	84.3

There are 10 PO_4^{3-} groups in a unit of HAP, two out of ten remain inside and eight at the periphery. In this study, the positively charged NOS molecules were most likely bound by weak electrostatic bonds within the hexagonal structure of the HAP nanoparticles. Binding occurred between the negative charges of the polarized NOS ends and the positively charged phosphate ions in the HAP. The release of NOS at pH 1.2 and 37 °C is shown in Figure 6. The releasing process has continued for 30 h. as the increasing manner and after 30 h it remained constant (10.28 ppm). The linearity equation was y=2.322x - 0922.

Genotoxicity tests are indispensable tests for the drug industry for the safety of new drugs. It is well-known that a large number of drugs cause oxidative stress. Oxidation on DNA results in various lesions such as basic zones and single or double helix fractures. It was earlier reported that a 15 mg/kg dose of NOS caused important chromosomal damage [50,51]. The aneugenicity of the NOS was also reported by Sheyd [52], and suggested being careful when using it in children and pregnant women. After half a decade of this report, Tiveron et al, [53] found the therapeutic dose of the NOS (EC_{50} 300 mg/kg). Since the suggested dose was high, a nano-capsulation was anticipated. Kumar et al. [45] showed that NOS has a non-carcinogenic structure with the Ames test. Acute toxicity lethal dosage value (LD50) was calculated as 2.469 mol/kg. The oral rat chronic toxicity score was analyzed as 1.451 log mg/kg BW/day.
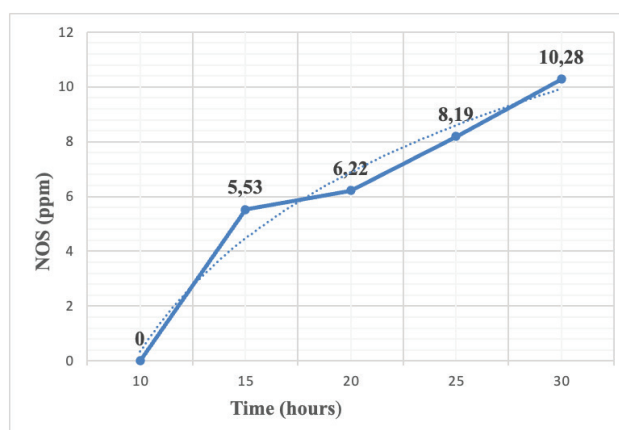
Figure 6. HPLC analysis results in vitro release profiles of HA nanoparticles loaded with Noscapine.

In this study, the genotoxic effect of NOS-loaded HAP (HAP+NOS) was evaluated by measuring the values of both comet and oxidative stress parameters (TAS, TOS, and OSI) (Table 4). In the studies of TAS and TOS level determination, when the concentration of the increase of the NOS increased total oxidant capacity and decreased the total antioxidant capacity. This rise and decline were found to be statistically significant at 10 and 25 mg/mL concentrations

Table 5. Detection of DNA damage by comet test and its relation to oxidative stress

Groups	Comet assay	Measurement of total oxidant status and oxidative stress index		
	DNA damage(ArbitraryUnit)* Mean±SD	TAS Mean±SD	TOS Mean±SD	OSI (AU) Mean±SD
Control	0.33±0.33a	19.14±3.15a	5.54±0.17a	3.54±0.17a
30 µM H₂O₂	271.67±4.37b	5.21±0.25b	19±4.25b	10.54±0.15b
25 mg/mL HA	110.67±2.33c	8.12±0.21e	14±1.23e	8.21±0.49e
10 mg/mL HA	8.33±0.67d	12±1.71d	10±1.51d	5.95±0.18d
5 mg/mL HA	1.67±0.33ae	16.57±0.41ac	7.01±1.11ac	4.52±0.6ac
25 mg/mL HA+NOS	7.67±0.67d	14.11±1.63c	9.33±1.33d	6.52±0.4d
10 mg/mL HA+NOS	2.33±0.58ae	16.25±3.10ac	6.15±4.12ac	5.32±0.4ac
5 mg/mL HA+NOS	1.33±0.33ae	17.78±3.16ac	5.78±2.12ac	4.41±0.1ac

* Means with the same letter in the same columns do not differ statistically at the level of 0.05; ppb: parts per billion; SD: Standard Deviation, HA: Hydroxyapatite, NOS: Noscapine, OSI; Quercetin equivalent.

of HAP alone and 25 mg/mL NOS-loaded HAP (p=0.005). These findings were concordant with the findings obtained from the Comet test, which showed evidence of the DNA breaks. As seen in Table 5, when we used NOS-loaded HAP, the oxidative stress was observed to be decreasing.

In cancer treatment, natural origin anticancer agents such as NOS that target microtubules show significant success in the treatment of patients. However, it justifies the search for new pharmaceutics with lower toxicity and higher efficacy, reducing the side effects of existing treatments. In light of the excellent antiviral and antimicrobial [54] properties of NOS-based compounds, research is needed to re-evaluate it as an anticancer drug.

Also, HAP has been identified as a promising material for biological applications. The distribution of several anticancer medicines via passive targeting has been studied using a variety of HAPs-based drug delivery systems [55-60]. However, there are few studies on utilizing hydroxyapatite nanostructures as a carrier for active targeted delivery of anticancer medicines [61-63]. Doxorubicin hydrochloride (DOX)-loaded HAP modified with hyaluronic acid. In mice with Heps xenografts, DOX-loaded HAPs demonstrated tumor-targeting capability as well as improved antitumor effectiveness [61]. A549 cells overexpressing CD44 were shown to have a preferential binding of polyethyleneimine coated hydroxyapatite nanoparticles modified with hydroxyapatite, as well as pH-responsive drug release [63].

CONCLUSION

To our knowledge, this is the first study that demonstrates the DNA damage efficacy of NOS-loaded HA nanoparticles. Hydroxyapatite appears to be an interesting alternative to future studies, considering the wide range of advantages of nanoparticles and the lack of study of NOS. Current studies are still not enough to revive the production of new products containing NOS-loaded nanoparticles in the pharmaceutical industry. Future studies should be about increasing the encapsulation efficiency and loading capacity of HAP NPs loaded with NOS and determining whether NOS loaded HAP NPs will be effective in cancer treatment with *in vivo* studies.

ACKNOWLEDGMENTS

AUTHORSHIP CONTRIBUTIONS

Authors equally contributed to this work.

DATA AVAILABILITY STATEMENT

The authors confirm that the data that supports the findings of this study are available within the article. Raw data that support the finding of this study are available from the corresponding author, upon reasonable request.

CONFLICT OF INTEREST

The author declared no potential conflicts of interest with respect to the research, authorship, and/or publication of this article.

ETHICS

There are no ethical issues with the publication of this manuscript.

REFERENCES

[1] Ke Y, Ye K, Grossniklaus HE, Archer DR, Joshi HC, Kapp JA. Noscapine inhibits tumor growth with little toxicity to normal tissues or inhibition of immune responses. Cancer Immunol Immunother 2000;49:217−225. [CrossRef]

[2] Jackson T, Chougule MB, Ichite N, Patlolla RR, Singh M. Antitumor activity of noscapine in human non-small cell lung cancer xenograft model. Cancer Chemother Pharmacol 2008;63:117−126. [CrossRef]

[3] Sood D, Kumar, N, Singh A, Tomar V, Dass SK, Chandra R. Deciphering the binding mechanism of noscapine with lysozyme: biophysical and chemoinformatic approaches. ACS Omega 2019;4:16233−16241. [CrossRef]

[4] Karna1 P, Rida PCG, Pannu V, Gupta KK, Dalton WB, Joshi H, et al. Novel microtubule-modulating noscapinoid triggers apoptosis by inducing spindle multipolarity via centrosome amplification and declustering. Cell Death Differ 2011;18:632−644. [CrossRef]

[5] Jayaraj RL, Beiram R, Azimullah S, Nagoor Meeran MF, Shreesh K, Ojha AA, et al. Noscapine prevents rotenone-ınduced neurotoxicity: Involvement of oxidative stress, neuroinflammation and autophagy pathways. Molecules 2021;26:4627. [CrossRef]

[6] Ebrahimi SA. Noscapine, a possible drug candidate for attenuation of cytokine release associated with SARS-CoV-2. Drug Dev Res 2020;26:765−767. [CrossRef]

[7] Mooraki A, Jenabi A, Jabbari M, Zolfaghari MI, Javanmardi SZ, Mahmoudian M, et al. Noscapine suppresses angiotensin converting enzyme inhibitors-induced cough. Nephrology 2005;10:348−350. [CrossRef]

[8] Mahmoudian M, Rezvani M, Rohani M, Benaissa F, Jalili M, Ghourchian S. A novel effect of noscapine on patients with massive ischemic stroke: A pseudo-randomized clinical trial. Iran J Neurol 2015;14:12−16.

[9] Vahabzadeh G, Rahbar-Roshandel N, Ebrahimi SA, Mahmoudian M. Neuroprotective effect of noscapine on cerebral oxygenglucose deprivation injury. Pharmacol Rep 2015;67:281−288. [CrossRef]

[10]   Yan AI, Kseniya YF, Rustam TM, Andrey KB, Alexey KB, Anastasiya AV, et al. Antibacterial activity of noscapine analogs. Bioorganic Med Chem Lett 2021;43:128055. [CrossRef]

[11]   Dahlstrom B, Mellstrand T, Lofdahl CG, Johansson M. Pharmacokinetic properties of noscapine. Eur J Clin Pharmacol 1982;22:535–539. [CrossRef]

[12]   Karlsson MO, Dahlstrom D, Eckernas SA, Johansson M, Tufvesson AT. Pharmacokinetics of oral noscapine. Eur J Clin Pharmacol 1990;39:275–279. [CrossRef]

[13]   Bitoun E, Micheloni A, Lamant L, Bonnart C, Tartaglia-Polcini A, Cobbold C, et al. LEKTI proteolytic processing in human primary keratinocytes, tissue distribution and defective expression in Netherton syndrome. Hum Mol Genet 2003;12:2417–2430. [CrossRef]

[14]   Sebak S, Mirzaei M, Malhotra M, Kulamarva A, Prakash S. Human serum albumin nanoparticles as an efficient Noscapine drug delivery system for potential use in breast cancer: preparation and in vitro analysis. Int J Nanomed 2010;5:525. [CrossRef]

[15]   Abdalla MO, Aneja R, Dean D, Rangari V, Russell A, Jaynes J, et al. Synthesis and characterization of Noscapine loaded magnetic polymeric nanoparticles. J Magn Magn Mater 2010;322:190–196. [CrossRef]

[16]   Kar F, Hacioglu C, Goncu Y, Sogut I, Senturk H, Donmez DB, et al. In vivo assessment of the effect of hexagonal boron nitride nanoparticles on biochemical, histopathological, oxidant and antioxidant status. J Clust Sci 2021;32:517–529. [CrossRef]

[17]   Kar F, Söğüt İ, Hacıoğlu C, Göncü Y, Şentürk H, Şenat A, et al. Hexagonal boron nitride nanoparticles trigger oxidative stress by modulating thiol/disulfide homeostasis, Hum Exp Toxicol 2021;40:1572–1583. [CrossRef]

[18]   Kun Z, Yong Z, Cong X, Wanlu Z, Hongfeng W, Jiaoqing T, et al. Application of hydroxyapatite nanoparticles in tumor-associated bone segmental defect. Appl Sci Eng 2019;5:1–16. [CrossRef]

[19]   Fu Q, Rahaman MN, Zhou N, Huang W, Wang D, Zhang L, et al. In vitro study on different cell response to spherical hydroxyapatite nanoparticles. J Biomater Appl 2008;23:37–50. [CrossRef]

[20]   Yuan Y, Liu C, Qian J, Wang J, Zhang Y. Size-mediated cytotoxicity and apoptosis of hydroxyapatite nanoparticles in human hepatoma HepG2 cells. Biomaterials 2010;31:730–740. [CrossRef]

[21]   Xu J, Xu P, Li Z, Huang J, Yang Z. Oxidative stress and apoptosis induced by hydroxyapatite nanoparticles in C6 cells. J Biomed Mater Res Part A 2012;100:738-745. [CrossRef]

[22]   Han Y, Li S, Cao X, Yuan L, Wang Y, Yin Y, et al. Different inhibitory effect and mechanism of hydroxyapatite nanoparticles on normal cells and cancer cells in vitro and in vivo. Sci Rep 2015;4:7134. [CrossRef]

[23]   Lu L, Li M, Li L, Wei S, Hu X, Wang X, et al. High-activity chitosan/nano hydroxyapatite/zoledronic acid scaffolds for simultaneous tumor inhibition, bone repair and infection eradication. Mater Sci Eng C 2008;82:225–233. [CrossRef]

[24]   Palazzo B, Sidoti MC, Roveri N, Tampieri A, Sandri M, Bertolazzi L, et al. Controlled drug delivery from porous hydroxyapatite grafts: An experimental and theoretical approach. Mater Sci Eng 2005;25:207–213. [CrossRef]

[25]   Gamez-Meza N, Noriega-Oriega-Rodriguez JA, Medina-Juarez LA, OrtegaGarcia J, Cazarez-Casanova R, Angulo-Guerrero O. Antioxidant activity in soybean oil of extracts from thompson grape bagasse. J Am Oil Chem 1999;76:1445. [CrossRef]

[26]   Chang C, Yang M, Wen H, Chern J. Estimation of total flavonoid content in propolis by two complementary colorimetric methods, J. Food Drug Anal 2002;10:178–182. [CrossRef]

[27]   Bulduk I, Taktak F. Isolation and Characterization of Antitumor Alkaloid from Poppy Capsules (Papaver somniferum). J Chem 2013;2013:493870. [CrossRef]

[28]   Kuriakose TA, Kalkura SN, Palanichamy M, Arivuoli D, Dierks K, Bocelli G, et al. Synthesis of stoichiometric nano crystalline hydroxyapatite by ethanol-based sol-gel technique at low temperature. J. Cryst Growth 2004;263:517–523. [CrossRef]

[29]   Ergün Y, Başpınar SM. Effect of acid passivation and H2 sputtering pretreatments on the adhesive strength of sol-gel derived Hydroxyapatite coating on titanium surface. Int J Hydrog Energy 2017;42:20420–20429. [CrossRef]

[30]   Gün M. Investigation of the use of alginate-chitosan nanoparticles in colchicine release (master thesis). Aydın: Adnan Menderes University, Institute of Science and Technology; 2013.

[31]   Singh H, Singh P, Kumari K, Chandra A, Dass SK, Chandra R. A review on noscapine, and its ımpact on heme metabolism. Curr Drug Metab 2013;14:351–360. [CrossRef]

[32]   Avuloğlu Y, Yüzbaşıoğlu D. Evaluation of genotoxic effects of 3-methyl-5-(4- carboxycyclohexyl-methyl)-tetrahydro-2H-1,3,5-thiadiazine-2-thione on human peripheral lymphocytes. Pharm Biol 2017;55:1228–1233. [CrossRef]

[33]   Ciğerci IH, Liman R, Özgül E, Konuk M. Genotoxicity of indium tin oxide by Allium and Comet tests. Cytotechnol 2015;67:157–163. [CrossRef]

[34]   Erel O. A novel automated direct measurement method for total antioxidant capacity using a new generation, more stable ABTS radical cation. Clin Biochem 2004;37:277–285. [CrossRef]

[35]   Erel O. A new automated colorimetric method for measuring total oxidant status. Clin Biochem 2005;38:1103–1111. [CrossRef]

[36] Zhaparova, L. Synthesis of nanoparticles and nano-capsules for controlled release of the antitumor drug "Arglabin" and antituberculosis drugs (doctorial thesis). Eindhoven: Technische Universiteit Eindhoven; 2012.

[37] Palmer LC, Newcomb CJ, Kaltz SR, Spoerke ED, Stupp SI. Biomimetic systems for hydroxyapatite mineralization inspired by bone and enamel. Chem Rev 2008;108:4754–4783. [CrossRef]

[38] Meyers MA, Chen PY, Lin AYM, Seki Y. Biological materials: structure and mechanical properties. Prog Mater Sci 2008;53:1–20. [CrossRef]

[39] Hui J, Wang X. Hydroxyapatite nanocrystals: colloidal chemistry, assembly, and their biological applications. Inorg Chem Front 2014;1:215–225. [CrossRef]

[40] Liu TY, Chen SY, Liu DM, Liou SC. On the study of BSA-loaded calcium-deficient hydroxyapatite nano-carriers for controlled drug delivery. J Control Release 2005;107:112–121. [CrossRef]

[41] Uskovic V, Uskovic DP. Nanosized hydroxyapatite, and other calcium phosphates: chemistry of formation and application as drug and gene delivery agents. J Biomed Mater Res 2011;96B:152–191. [CrossRef]

[42] Lafisco M, Delgado-Lopez JM, Varoni EM, Tampieri A, Rimondini L, Gomez-Morales J, et al. Cell surface receptor targeted biomimetic apatite nanocrystals for cancer therapy. Small 2013;25:3834–3844. [CrossRef]

[43] Dumontet C, Jordan MA. Microtubule-binding agents: a dynamic field of cancer therapeutics. Nat Rev Drug Discov 2010;9:790–803. [CrossRef]

[44] Kumar N, Sood D, Spek PJ, Sharma HS, Chandra R. Molecular binding mechanism and pharmacology comparative analysis of noscapine for Repurposing against SARS-CoV-2 protease. J Proteome Res 2020;19:4678–4689. [CrossRef]

[45] Feng W, Li MS, Lu YP, Qi YX, Liu YX. Synthesis and microstructure of hydroxyapatite nanofibers synthesized at 37°C. Mater Chem Phys 2006;95:145–149. [CrossRef]

[46] Cengiz B. Hidroksiapatit nanoparçacıklarının sentezi (yüksek lisans tezi). Ankara: Ankara Üniversitesi Kimya Mühendisliği Anabilim Dalı, Fen Bilimleri Enstitüsü, 2007.

[47] Kong L, Mu Z, Yu Y, Zhang L, Hu J. Polyethyleneimine stabilized HAPs modified with hyaluronic acid for targeted drug delivery. RSC Adv 2017;6:101790–101799. [CrossRef]

[48] Langit KS, Auerkaria EI. Genotoxicity and repair capability of DNA following the oral exposure to analgesic drugs: A review. AIP Conference Proceed 2021:2344. [CrossRef]

[49] Schuler M, Muehlbauer P, Guzzie P, Eastmond DA. Noscapinehydrochloride disrupts the mitotic spindle in mammalian cells and induces aneuploidy as well as polyploidy in cultured human lymphocytes. Mutagenesis 1999;14:51–56. [CrossRef]

[50] Gatehouse DG, Stemp G, Pascoe S, Wilcox P, Hawker J, Tweats DJ. Investigations into the induction of aneuploidy and polyploidy in mammalian cells by the anti-tussive agent noscapine hydrochloride. Mutagenesis 1991;6:279–283. [CrossRef]

[51] Sneyd JR. Papaveretum in women of childbearing potential. BMJ 1991;303:852. [CrossRef]

[52] Tiveron MC, Hirsch MR, Brunet JF. The expression pattern of the transcription factor Phox2 delineates synaptic pathways of autonomous nervous. J Neurosci 1996;16:7649–7660. [CrossRef]

[53] Nemati F, Bischoff-Kont I, Salehi P, Nejad-Ebrahimi S, Mohebbia M, Bararjanian M, et al. Identification of novel anti-cancer agents by the synthesis and cellular screening of a noscapine-based library. Bioorganic Chem 202;115:105135. [CrossRef]

[54] Yang YH, Liu CH, Liang YH, Lin FH, Wu KCW. Hollow mesoporous hydroxyapatite nanoparticles (hmHANPs) with enhanced drug loading and pH-responsive release properties for intracellular drug delivery. J Mater Chem B 2013:2447–2450. [CrossRef]

[55] Chen M, Feng W, Lin S, He C, Gao Y, Wang H. Antitumor efficacy of a PLGA composite nanofiber embedded with doxorubicin@MSNs and hydroxycamptothecin@ HANPs. RSC Adv 2014;95:53344–53351. [CrossRef]

[56] Li D, He J, Huang X, Li J, Tian H, Chen X, et al. Intracellular pH-responsive mesoporous hydroxyapatite nanoparticles for targeted release of anticancer drug. RSC Adv 2015;5:30920–30928. [CrossRef]

[57] Xu S, Shi J, Feng D, Yang L, Cao S. Hollow hierarchical hydroxyapatite/Au/ polyelectrolyte hybrid microparticles for multi-responsive drug delivery. J Mater Chem B 2014;2:6500–6507. [CrossRef]

[58] Verma G, Barick KC, Shetake NG, Pandey BN, Hassan PA. Citrate-functionalized hydroxyapatite nanoparticles for pH-responsive drug delivery. RSC Adv 2016;6:77968–77976. [CrossRef]

[59] Verma G, Shetake NG, Barick KC, Pandey BN, Hassan PA, Priyadarsini KI. Covalent immobilization of doxorubicin in glycine functionalized hydroxyapatite nanoparticles for pH-responsive release. New J Chem 2018;42:6283–6292. [CrossRef]

[60] Xiong H, Du S, Ni J, Zhou J, Yao J. Mitochondria and nuclei dual-targeted heterogeneous hydroxyapatite nanoparticles for enhancing the therapeutic efficacy of doxorubicin. Biomaterials 2016;94:70–83. [CrossRef]

[61] Lee MS, Lee JE, Byun E, Kim NW, Lee K, Lee H, et al. Target-specific delivery of siRNA by stabilized calcium phosphate nanoparticles using dopa-hyaluronic acid conjugate. J Control Release 2014;192:122–130. [CrossRef]

[62] Kong L, Mu Z, Yu Y, Zhang L, Hu J. Polyethyleneimine-stabilized hydroxyapatite nanoparticles modified with hyaluronic acid for targeted drug delivery. RSC Adv 2016;6:101790−101799. [CrossRef]

[63] Qiu C, Wei W, Sun J, Zhang HT, Ding JS, Wang JC, et al. Systemic delivery of siRNA by hyaluronan-functionalized calcium phosphate nanoparticles for tumor-targeted therapy. Nanoscale 2016;26:13033−13044. [CrossRef]